Microbial Architecture of Environmental Sulfur Processes: A Novel Syntrophic Sulfur-Metabolizing Consortia

KELSEY L.I. NORLUND,[†] GORDON SOUTHAM,[‡] TOLEK TYLISZCZAK,[§] YONGFENG HU,[∥] CHITHRA KARUNAKARAN,[∥] MARTIN OBST,[∥,⊥] ADAM P. HITCHCOCK,[⊥] AND LESLEY A. WARREN*[,†]

School of Geography and Earth Sciences, McMaster University, Hamilton, Ontario, L8S 4K1 Canada, Department of Earth Sciences, University of Western Ontario, London, Ontario N6A 5B7, Canada, Advanced Light Source, Lawrence Berkeley National Laboratory, Berkeley, California 94720, Canadian Light Source, Inc., University of Saskatchewan, Saskatoon, Saskatchewan S7N 5C6, Canada, and Brockhouse Institute for Materials Research and Departmentof Chemistry, McMaster University, Hamilton, Ontario L8S 4M1, Canada

Received December 19, 2008. Revised manuscript received June 25, 2009. Accepted July 9, 2009.

Microbial oxidation of sulfur-rich mining waste materials drives acid mine drainage (AMD) and affects the global sulfur biogeochemical cycle. The generation of AMD is a complex, dynamic process that proceeds via multiple reaction pathways. The role of natural consortia of microbes in AMD generation, however, has received very little attention despite their widespread occurrence in mining environments. Through a combination of geochemical experimentation and modeling, scanning transmission X-ray microscopy, and fluorescent in situ hybridization, we show a novel interdependent metabolic arrangement of two ubiquitous and abundant AMD bacteria: chemoautotrophic sulfur-oxidizing *Acidithiobacillus* sp. and heterotrophic *Acidiphilium* sp. Highly reminiscent of anaerobic methane oxidation (AOM) consortia, these bacteria are spatially segregated within a planktonic macrostructure of extracellular polymeric substance in which they syntrophically couple sulfur oxidation and reduction reactions in a mutually beneficial arrangement that regenerates their respective sulfur substrates. As discussed here, the geochemical impacts of microbial metabolism are linked to the consortial organization and development of the pod structure, which affects cell−cell interactions and interactions with the surrounding geochemical microenvironment. If these pods are widespread in mine waters, echoing the now widespread discovery of AOM consortia, then AMD-driven CO_2 atmospheric fluxes from H_2SO_4 carbonate weathering could be reduced by as much as 26 TgC/yr. This novel sulfur consortial discovery indicates that organized metabolically linked microbial partnerships are likely widespread and more significant in global elemental cycling than previously considered.

Introduction

Understanding observed biogeochemical cycles in the environment hinges on understanding complex microbial interactions within communities and with the environmental niches in which these communities occur (*1*−*3*). Acid-consuming and acid-generating sulfur reactions may be catalyzed by microbial communities and are interdependent on environmental conditions, sulfur substrate, and the microbial consortia involved (*4, 5*). Each reaction pathway has different potential impacts on water quality, including acid generation in acid mine drainage (AMD) environments as well as influencing the global sulfur biogeochemical cycle. To date, these microbial reaction pathways remain poorly elucidated, reflecting the complexity of the pathways involved and analytical challenges associated with the characterization of many intermediate oxidation state sulfur species (*4*).

The identification of the microbial partners in the marine anaerobic methane oxidation (AOM) consortium (*6*) demonstrated interdependent metabolisms of spatially segregated bacterial sulfate reducers and archeal anaerobic methane oxidizers associated with a repeatable macrostructure. Syntrophic and linked metabolisms in microbial communities have also been shown for anaerobic ammonia oxidation (ANAMOX, ref *7*) and interspecies hydrogen transfer (*8*). While still poorly characterized, given the energetic possibilities of syntrophic metabolisms and the ecological advantages for their occurrence, these described consortial discoveries underscore the likelihood that other as yet unidentified environmental microbial partnerships are involved in global elemental cycles.

Discoveries of such novel microbial consortia are more likely for elemental cycles where microbial activity is implicated, and current geochemical models do not capture observed behavior accurately. Acid mine drainage (AMD) is a globally significant mining water quality issue that is largely driven by microbially catalyzed sulfur oxidation reactions (*9, 10*) carried out by chemolithoautotrophic bacteria during their metabolic fixation of CO_2. Estimates of AMD sulphuric acid generation assume (1) abiotic, oxygen-driven, and complete oxidation of the reduced sulfur in mine waste rock and tailings to sulfate, SO_4^{2-} (eq 1) and (2) AMD-generated acid flux $[H^+]$ is proportional to measured aqueous sulfate concentrations $[SO_4^{2-}]$ (eq 1 and refs *11, 12)*

$$FeS_2 + 7.5O_2 + H_2O \rightarrow 2SO_4^{2-} + 4H^+ + Fe(OH)_3 \quad (1)$$

Although geochemical modeling of AMD acid generation is predicated upon the complete oxidation of reduced sulfur (eq 1), sulfur can exist in multiple oxidation states in the environment from sulphide, $\sum H_2S$, ($S^{(-II)}$) to sulfate, ($S^{(+VI)}$). The eight electron difference between these two end members requires multiple reaction pathways across a series of sulfur oxidation intermediates (anything of lower oxidation state than sulfate and higher oxidation state than sulphide) when mediated by microbial activity. Thus, AMD autotrophic sulfur and iron-oxidizing bacteria process sulfur through a series of reactions involving intermediate sulfur species before final oxidation to sulfate (*4, 5, 9*), which decouples the observed sulfate concentrations from acid generation associated with eq 1. Furthermore, microbial sulfur reactions

* Corresponding author phone: +1 905 525-9140, ext. 27347; fax: +1 905 546 0463; e-mail: warrenl@mcmaster.ca.
[†] School of Geography and Earth Sciences, McMaster University.
[‡] University of Western Ontario.
[§] Lawrence Berkeley National Laboratory.
[∥] University of Saskatchewan.
[⊥] Brockhouse Institute for Materials Research and Departmentof Chemistry, McMaster University.

10.1021/es803616k CCC: $40.75
Published on Web 07/21/2009

can include disproportionation pathways, which produce lower oxidation states of sulfur through acid-consuming reactions (*4, 5*). Laboratory investigation of AMD microbial sulfur geochemistry driven by the mine bacterial enrichment used in this study confirmed the importance of disproportionation reactions (*4, 5*). The production of thiosulphate ($S_2O_3^{2-}$), sulfate, and colloidal elemental sulfur (S^0) occurred when tetrathionate ($S_4O_6^{2-}$), a key sulfur intermediate produced during microbial oxidation of pyritic mining waste (*13*), was used as the starting substrate (eq 2 and ref *4*). These microbially produced sulfur oxidation intermediates may then be further metabolized and/or disproportionated through a series of interlinked reactions by microbial activity (eqs 3−5 and ref *14*), increasing the discrepancies between measured [SO_4^{2-}] and estimated [H^+] used in AMD models.

$$S_4O_6^{2-} + H_2O \rightarrow S_2O_3^{2-} + SO_4^{2-} + S^0_{colloidal} + 2H^+ \quad (2)$$

$$nS_2O_3^{2-} + (n-1)H^+ \rightarrow HS_nSO_3^- + nHSO_3 \quad (3)$$

$$HS_nO_3^- + 1.5O_2 \rightarrow S_nO_6^{2-} + H^+ \quad (4)$$

$$2S_2O_3^{2-} + 4H^+ + O_2 \rightarrow S_4O_6^{2-} + 2H_2O \quad (5)$$

In this study, we determine the linkages between observed AMD microbial sulfur biogeochemistry and the microbial ecology associated with these reactions. We use a combination of transmission electron microscopy (TEM), scanning transmission X-ray microscopy (STXM), and fluorescent in situ hybridization (FISH) techniques to develop a sulfur biogeochemical model identifying the important microbial players, sulfur reactions, and microbial ecology.

Materials and Methods

Microbial Environmental Enrichment and Phylogenetic Analysis. Microbial tetrathionate oxidation batch experiments were performed with an environmental microbial enrichment collected from a mine tailings oxidation pond (Moose Lake, Xstrata Nickel, Onaping, ON; pond characterized in ref *10*). Stable enrichments were maintained in autoclaved 250 mL flasks with filter-sterilized (0.22 μm pore size) minimal salts media with tetrathionate as the sulfur source and no carbon added (*4*): $(NH_4)_2SO_4$ 0.2 g/L, $MgSO_4$ 0.25 g/L, $CaCl_2 \cdot 2H_2O$ 0.36 g/L, KH_2PO_4 0.5 g/L, $FeSO_4$ 10 mg/L, and $K_2S_4O_6^{2-}$ 5 g/L. Flasks were covered with a double-layer of aluminum foil to allow gas diffusion and kept static on the laboratory bench. The initial pH of the enrichments was 4 ± 0.05, and enrichments were incubated at room temperature (approximately 22 °C). Throughout the time course of this experiment, the pH decreased due to sulphuric acid generation to a final pH of approximately 2.

The phylogeny of the microbial community was determined by 16S rRNA analysis. Total DNA was extracted using the PowerSoil DNA Isolation Kit (Mo Bio Laboratories, Carlsbad, CA) from filtered solids (>0.22 μm) following the manufacturer-supplied protocols. The DNA sample was amplified by the polymerase chain reaction (PCR) using the universal 16S rDNA primers 515F and 1391R. Sequencing was completed with ABI BigDye terminator chemistry, using a 3730 DNA analyzer (Applied Biosystems, Foster City, CA and Institute for Molecular Biology and Biotechnology, McMaster University, ON, Canada). Sequences for 28 clones were compared to GenBank nucleotide databases using the Basic Local Alignment Search Tool (BLAST) software. Greater than 97% similarity was used to define membership in a microbial species.

Optical Microscopy. Reflection images of the pods and deposits dried on silica nitride (Si_3N_4) windows (Norcada) were recorded in air with 20x, 50x and 100x objectives using a Leica DMR microscope.

Transmission Electron Microscopy (TEM). Samples for TEM were preserved in 2.5% glutaraldehyde, adsorbed to Formvar carbon-coated 200 mesh Cu grids, and examined at 80 kV using a Philips CM-10 transmission electron microscope.

Scanning Transmission X-ray Microscopy (STXM). STXM spectromicroscopy (imaging at a sequence of photon energies at the S 1s, S 2p, and C 1s edges(refs *15, 16)* identified and mapped the sulfur and organic chemical components of three pods at a 30 nm spatial resolution. X-ray imaging and spectromicroscopy studies were carried out at the STXMs (*17*) on beamline 10ID1 (*18*) at the Canadian Light Source (CLS, Saskatoon, SK, Canada) and on beamlines 5.3.2 (*19*) and 11.0.2 (*20*) at the Advanced Light Source (Berkeley, CA).

Sulfur oxidation states in the environmental microbial enrichment were determined by measuring the S 2p spectra of the aggregates and smaller scale deposits in contact with microbial aggregates. The S 2p spectra were identified using reference compounds measured at the CLS PGM beamline or from literature values (*21*).

Fluorescent in Situ Hybridization (FISH). Fluorescent in situ hybridization (FISH) analysis was performed using the genus-specific molecular probes Thio820 (ACCAAACATCTAGTATTCATC 5′-labeled Texas Red, *Acidithiobacillus*) and Acdp821 (AGCACCCCAACATCCAGCACACAT 5′-labeled Alexafluor488, *Acidiphilium*; ref *22*). Fluorescent imaging of greater than 50 pods was performed with a Leica LEITZ DMRX epifluorescent microscope [Leica Microsystems (Canada), Richmond Hill, ON] using TX2 (*Acidithiobacillus*) and K3 (*Acidiphilium*) filters. Openlab 2.2.5 (Improvision, Coventry, U.K.) was used for digital imaging. Adobe Photoshop version 6.0 was used to overlay images and adjust brightness and contrast.

Results and Discussion

Sulfur Biogeochemistry of Planktonic Microbial Aggregates ("Pods"). Optical microscopy of the AMD sulfur-oxidizing enrichment indicated the occurrence of small planktonic aggregates of cells encased within extracellular polymeric substance (EPS, "pods") suspended in the enrichment media (Figure 1a). TEM coupled with energy dispersive X-ray (EDX) spectroscopy demonstrated the presence of colloidal sulfur associated with the cells and the surrounding EPS pod macrostructure (Figure 1b and Figure S1 of the Supporting Information). The microbial production and subsequent metabolism of colloidal elemental sulfur (microbial sulfur) that is physically distinct from abiotic elemental sulfur is known (*14, 23−25*), although the mechanisms for production, uptake, and metabolism of microbial sulfur by AMD microorganisms are not well understood. The production and subsequent use of colloidal sulfur has been previously demonstrated for this environmental enrichment (*4, 5*).

Analyses of STXM image sequences of the EPS cell aggregates at the C 1s edge clearly showed that bacterial cells and their associated matrix of extracellular polymeric substances (EPS, Figure 1c,d) form a repeatable macrostructure that is consistent across pods. X-ray absorption spectroscopy studies of microbial sulfur have been performed previously and suggest that the reduced sulfur produced by AMD bacterium *Acidithiobacillus ferrooxidans* is some combination of elemental sulfur (ring and polymeric structure), polythionates, and possibly organo−sulfur compounds (*25, 26*). To our knowledge, the S 1s study at the CLS STXM is the first report of a spectromicroscopy study at the S 1s energy range (2450−2500 eV) on a STXM based on a grazing incidence monochromator beamline, although S 1s spectra from this beamline have been reported elsewhere (*18*). The S 1s near-edge X-ray absorption fine structure (NEXAFS)

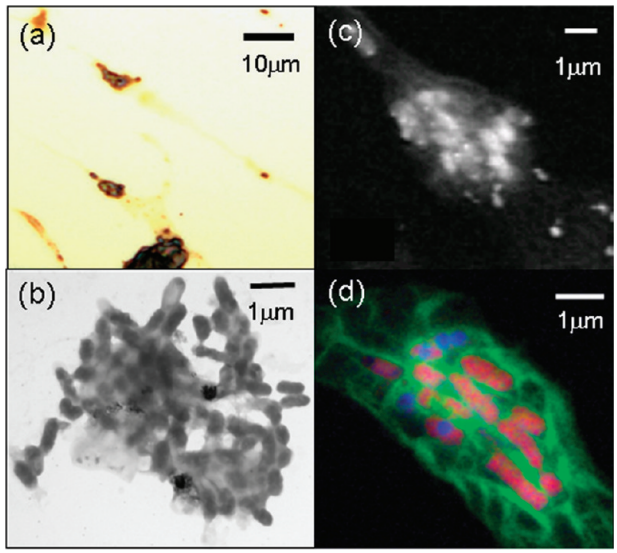

FIGURE 1. Multiple imaging techniques demonstrated the role of planktonic pods composed of extracellular polymeric substance (EPS) and microbial cells in sulfur processing. (a) Suspended pods and associated deposits were first located by optical imaging (reflection) of solution air-dried on a silicon nitride window. (b) Transmission electron microscopy of a pod shows the association of colloidal sulfur with the organic EPS phase, highlighting the role of the pod in particulate sulfur capture. (c) Scanning transmission X-ray microscopy (STXM) image at 176 eV (in optical density representation) indicates the arrangement of cells within the EPS macrostructure as well as excreted particles later identified as sulfate. (d) Color-coded composite map of polysaccharides in the EPS (green), protein of cell membranes (red), and lipid structures (blue) derived from a C 1s STXM image sequence of a pod.

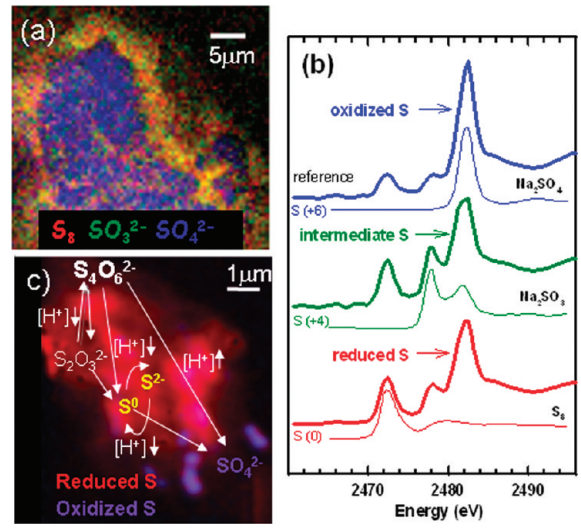

FIGURE 2. (a) Color-coded composite of the component maps for three sulfur oxidation states: reduced (fit to S_8, red), intermediate (fit to SO_3^{2-}, green), and oxidized (fit to SO_4^{2-}, blue), derived from a S 1s image sequence of a deposit from the environmental enrichment. Multiple oxidation states were simultaneously present, with the dominant oxidized form fully enclosed in reduced forms of S. (b) S 1s spectra of the pixels identified by the color-coded insert are compared to reference spectra for S(0) (elemental sulfur), S(+4) (sodium sulphite), and S(+6) (sodium sulfate). Observed sulfur species are those predicted from tetrathionate disproportionation (eq 1). (c) Color-coded composite of maps of reduced sulfur (red) and oxidized sulfur (blue), derived from a S 2p STXM image sequence, indicates that the microbial sulfur pathways being catalyzed by these pods included acid consumption through disproportionation reactions (eqs 2–5).

spectra of sulfur-rich deposits produced by the enrichment identified oxidized and reduced species of sulfur, consistent with microbial disproportionation of tetrathionate (Figure 2 and eq 2). The sulfur oxidation states of the pods and smaller scale deposits in contact with microbial aggregates were determined by comparison of the S 1s spectra with the S 1s spectra of suitable reference materials (Figure 2b) and verified at the S 2p edge (Figure S2 of the Supporting Information and ref *19*). The spectroscopic results confirmed that the reduced sulfur is a combination of zero-valent sulfur (consistent with microbial colloidal sulfur, S^0) and $S_2O_3^{2-}$, which are the predicted products of microbial tetrathionate disproportionation (eq 2). STXM results show that the reduced sulfur was specifically associated with the cells in the pods, and active metabolism of sulfur was evidenced by the simultaneous occurrence of multiple sulfur oxidation species (Figure 2c).

Results of our multitechnique imaging approach assessing multiple pods demonstrate the repeatability of pod size and shape (Figures 1–3). We propose that the pod macrostructure is ecologically and geochemically highly significant and occurs in a nonrandom manner. The pods occur suspended in bulk solution providing the pod bacteria access to fresh tetrathionate and oxygen supplies and facilitating microbial metabolism of tetrathionate. Excretions from the pods were identified as oxidized sulfur (sulfate, SO_4^{2-}), which is consistent with active pod microbial sulfur processing and disposal of a waste product (SO_4^{2-}) that is no longer metabolically accessible to sulfur-oxidizing bacteria (Figure 2). The bacterial use of organic compounds to colonize and capture S^0 has been shown previously (*27*), but the pods reported here identify a new cooperative strategy involving the formation of an EPS network surrounding an aggregate of cells that generates and collects colloidal S^0 providing a storage mechanism for this sulfur substrate.

Microbial Community Composition and Pod Structure–Function Dynamics. To identify the microbial players involved in the observed sulfur biogeochemistry and pod formation, we evaluated the phylogenetic composition of the bulk enrichment microbial community using 16S rRNA (rRNA) gene sequences. The microbial community was determined to include clones identified as *Acidiphilium* sp. DBS4–1 (an autotrophic sulfur oxidizer and a facultative heterotrophic elemental sulfur (S^0) reducer) (*28*), *Acidithiobacillus ferrooxidans* (a chemoautotrophic iron and sulfur oxidizer), and heterotrophic mycobacteria that are widespread in the environment (Table S1 of the Supporting Information). Fluorescent in situ hybridization (FISH) phylogenetic analyses of the experimental systems in this study revealed that the sulfur-processing pods contained two strains of microbes that hybridized with the genus-specific probes for *Acidithiobacillus* (Thio820) or *Acidiphilium* (Adcp821; Figure 3 and ref *22*). All the pods examined consisted of both bacterial species, indicating a nonrandom association of both strains and an ecological relationship. The pods showed a defined spatial organization of the two strains that consisted of an external layer of *A. ferrooxidans* surrounding an interior core of *Acidiphilium* spp. (Figure 3). While the literature reports the common co-occurrence of these two strains in AMD environments (*29, 30*), this is the first time that *A. ferrooxidans* and *Acidiphilium* spp. have been shown to occur in these regularized consortial arrangements. Furthermore, we are able to induce identical pod formation in laboratory experiments with pure strain type-cultures of *A. ferrooxidans* (ATCC 19859) and *Acidiphilium cryptum*

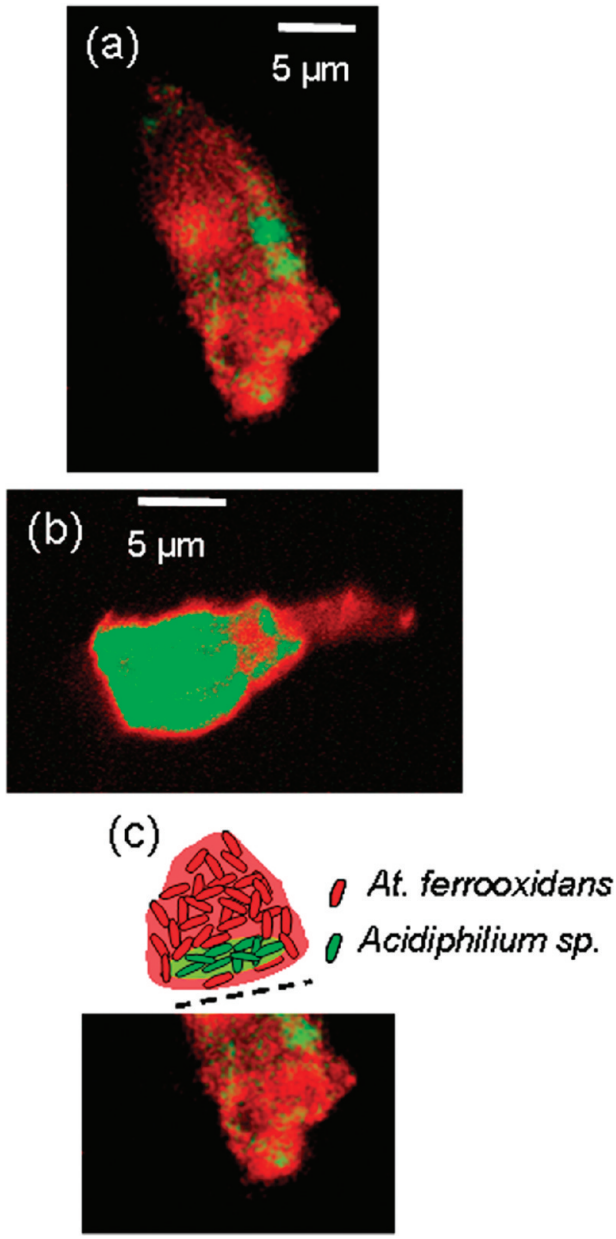

FIGURE 3. Fluorescent in situ hybridization (FISH) analysis using microbe-binding probes specific to *Acidithiobacillus* (Thio820, red) and *Acidiphilium* spp (green). (a) Specific spatial arrangement of the two strains observed with *Acidithiobacillus* (red) located in the outer layers of the pods surrounding a core of *Acidiphilium* (green). (b) Depth slicing through the pod shows the internal core of *Acidiphilium* (green). (c) Schematic model of the arrangement of the two bacterial strains within the pods.

(ATCC 33463), indicating that the pod structure is an important component to linked metabolism for these two bacteria.

Whether both strains are involved in the creation of the EPS pod is not known; however, their repeated pattern of association within a pod of regularized size and morphology strongly suggests that the structure of both the macro pod and the specific segregation of the two strains within the pod are linked to co-ordination of their sulfur metabolisms for mutual benefit. We propose that the regular morphology of the pod confers a configurational functionality that allows the maintenance of the internal geochemical conditions required to carry out cyclical sulfur redox reactions within a bulk oxygenated solution (Figure 4). As shown in eq 2 and confirmed by our STXM results (Figure 2), colloidal S^0 is produced when bacteria disproportionate aqueous tetrathionate. Both strains are capable of autotrophic sulfur oxidation; however *Acidiphilium* sp. DBS4−1 is also capable of heterotrophic S^0 reduction (*28*). *A. ferrooxidans* is a strict iron and sulfur oxidizer and presumably outcompetes the metabolic generalist *Acidiphilium* in autotrophic sulfur metabolism. Our multiple lines of evidence show that this consortium uses the pod structure to partition sulfur metabolism. Our results are consistent with mediation of autotrophic tetrathionate disproportionation producing colloidal S^0 (Figure 2 and eq 2) by *A. ferrooxidans* in the exterior layers of the pod where fresh supplies of tetrathionate from solution are available. The location of *Acidiphilium* specifically in the interior of the pod, where more reducing conditions can be maintained, is most consistent with heterotrophic metabolism by *Acidiphilium*, coupling the reduction of S^0 to sulphide, (ΣH_2S), to the oxidation of organic molecules (Figure 4b and eq 6). *Acidiphilium* would also serve another important role by removing the organic byproduct of autotrophic CO_2 fixation that may inhibit metabolism in *A. ferrooxidans*, as has been suggested for iron-grown strains of these bacteria (*30, 31*). The produced sulphide provides a new source of reduced sulfur which may be abiotically or microbially reoxidized to S^0 regenerating this sulfur source for *Acidiphilium* (Figure 4b and eq 7). Anecdotally sulphide was occasionally detectable by smell in the aerobic enrichments in the laboratory, providing evidence of its production by microbial activity. Sulphide undergoes rapid abiotic oxidation with only small concentrations of oxygen, which precluded its stability and thus detection under the conditions used for STXM analyses.

$$\begin{gathered} HCOOH + S^0 \rightarrow CO_2 + H_2S \\ \Delta G^\circ = -41.6\ kJ/molS \end{gathered} \tag{6}$$

$$\begin{gathered} S^{2-} + 2H^+ + \frac{1}{2}O_2 \rightarrow S^0 + 2H_2O \\ \Delta G^\circ = -151.4\ kJ/molS \end{gathered} \tag{7}$$

The partitioning of sulfur metabolism within the pods is advantageous to both strains since they would then not be directly competing for the same metabolic niche: sulfur oxidation. Rather, enabled by the pod macrostructure, they create a microbially controlled sulfur cycle, whereby each microbial strain regenerates its partner's respective sulfur substrate (either S^0 or ΣH_2S) through the cycled oxidation and reduction of the pod trapped colloidal S^0. This syntrophic metabolic relationship extends the metabolic lifetimes of the sulfur sources for both strains. Pods are observed to fall apart on cell death indicating that energy is required to maintain this structure and supporting the notion that the pod structure is important to create the necessary conditions required for their metabolically linked sulfur redox cycling.

These pods are the first to be specifically demonstrated for sulfur cycling. However, they reveal another unanticipated cooperative consortium linked to a global elemental cycle that is highly reminiscent of the structure−function dynamics reported for the marine AOM consortia (*6*). The pod associated coupled sulfur cycling reduces both sulfate generation as well as associated acid generation (i.e., protons, eq 2−7). Oxidation of reduced sulfur minerals (e.g., pyrite, FeS_2) due to mining activities and natural weathering processes has been estimated to release 2.4 Tmol S/year as oxidized sulfate and thus an estimated 4.8 Tmol H^+/year assuming complete aerobic oxidation to sulfate (eq 1). We have previously shown that the terminal electron acceptor (e.g., O_2 or ferric iron, Fe^{3+}) used by microbes in autotrophic sulfur metabolism controls the

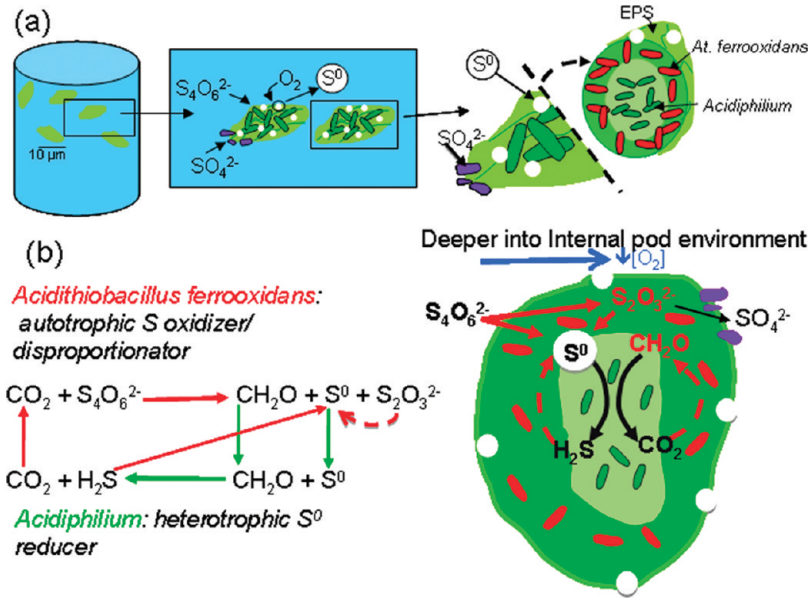

FIGURE 4. Proposed schematic of syntrophic sulfur processing in the multistrain pod. (a) The microbial pods occur pelagically in aerobic solution where they have access to fresh supplies of $S_4O_6^{2-}$. They carry out sulfur redox reactions enabled by the specific pod structural arrangements of the two bacterial strains within the pod, thereby capturing S^0 for subsequent metabolic use and as confirmed by S STXM results (Figure 2). (b). Proposed schematic of the metabolic sulfur redox linkages between *A. ferrooxidans* and *Acidiphilium* in the pod enabled by control of the internal pod microgeochemical environment. *A. ferrooxidans* disproportionates the $S_4O_6^{2-}$ producing $S_2O_3^{2-}$ and S^0. *Acidiphilium* then uses the S^0 heterotrophically to reduce organic carbon byproduct of *A. ferrooxidans* and produce H_2S. *Acidiphilium* occurs within the core of the pod where more reducing conditions can be maintained enabling favorable thermodynamics for sulfur reduction. This H_2S may be either abiotically or microbially reoxidized by *A. ferrooxidans,* thereby regenerating S^0. This cycling of sulfur maintains lower oxidative state forms accessible to both strains through a cooperative strategy.

relative importance of disproportionation (acid-consuming) and oxidation (acid-producing) reactions (*5*). Prior results of laboratory investigations of the environmental AMD enrichment described in this study showed that the increased disproportionation associated with iron-driven microbial sulfur metabolism consumed up to 90% of acid predicted from observed [SO_4^{2-}], assuming eq 1 as the dominant pathway (*5*). In O_2-driven systems, 40% less acid was produced than would be expected from eq 1 (*4, 5*). Consistent with the consortial sulfur recycling shown here, lower rates of pyrite oxidation have been reported when both *Acidiphilium* sp. and *Acidithiobacillus* sp. were present, compared to those observed for pyrite oxidation by only *Acidithiobacillus* sp. (*31*). Our results showing recycling of sulfur by this consortium maintaining lower oxidation state sulfur species provide an explanation for the observed lower SO_4^{2-} concentrations in that study's consortial treatments. In AMD environments, where Fe^{3+} concentrations are commonly high, microbially mediated sulfur cycling, as demonstrated in this study, will decrease expected net acid generation.

A widespread global occurrence of these consortial pods in AMD environments is highly plausible. Although the pod structure described here has not been identified in mining environments, *Acidithiobacillus* and Acidiphilium spp. are frequently identified together in mining microbial communities (*29*). *Acidiphilium* has been isolated from supposedly pure cultures of iron-grown *A. ferrooxidans* (*30*), and a mutualistic relationship between them has been previously suggested in iron cycling (*29*). This is the first study to provide evidence of their linked metabolisms and identify this cooperative strategy specifically in sulfur cycling. In a future communication, we will also report identical pod formation to those observed for our environmental AMD enrichment with pure strains of these two bacteria in the laboratory as well as conditions under which pods do not form, indicating the geochemical niches of these pods and confirming their likely occurrence across mine systems. We calculate that this cooperative microbial sulfur metabolic strategy could prevent as much as 1.2−3.7 Tmol of acid (H^+) release into the environment each year on the basis of the calculations discussed subsequently. Such a reduction in sulphuric acid (H_2SO_4) release has potential significant implications for global carbon fluxes associated with silicate and carbonate mineral weathering, which play key roles in modulating global climate. Net CO_2 sequestration associated with H_2CO_3 weathering is estimated at 70 TgC/yr (*11*), which is offset by an estimated 29 TgC/yr due to CO_2 release by AMD-derived H_2SO_4 carbonate weathering (*11*). The mechanisms identified in this work indicate that current model estimates of CO_2 atmospheric inputs associated with AMD-derived H_2SO_4 carbonate weathering overestimate acid generation when microbial sulfur reactions are considered. We estimate that the net atmospheric CO_2 release associated with AMD-derived H_2SO_4 carbonate weathering would be reduced by 11−26 TgC/yr with these microbial S recycling reactions (value depends on whether the terminal electron acceptor is O_2 or Fe^{3+}). Consequently, CO_2 release associated with H_2SO_4 weathering of carbonate minerals may be of substantially less concern than has previously been stated (*11, 12*).

In summary, we have provided evidence for a novel syntrophic microbial cooperative involved in global sulfur cycling that is highly reminiscent of the structure−function relationships observed for the marine AOM consortia (*6*). As these sulfur pod cooperatives create internal redox conditions that differ from bulk solution, their discovery and impacts can only be discerned by the combination of imaging, geochemical, and STXM characterization employed here. We believe that these types of microbial partnerships are likely to be more widespread in global elemental cycles than currently appreciated. They further underscore the importance of cooperative linked metabolism by microbial con-

sortia in environmental processes. Finally, they provide a highly promising new avenue to more fully understand the global processes controlling the environmental conditions of our planet.

Acknowledgments

Research is supported by the Natural Sciences and Engineering Research Council of Canada (NSERC) and Canada Research Chairs Program, Canada Foundation for Innovation (CFI). TEM was performed in the CFI-Ontario Innovation Trust (OIT)-funded Biotron at the University of Western Ontario. The S 1s STXM and S 2p spectroscopy described in this paper were performed in part at the Canadian Light Source, which is supported by NSERC, National Research Council (NRC), Canadian Institutes of Health Research (CIHR), and the University of Saskatchewan. STXM was also measured at beamlines 5.3.2 (C 1s) and 11.0.2 (S 2p) at the Advanced Light Source, Lawrence Berkeley National Lab, which is supported by the Division of Basic Energy Sciences of the U.S. Department of Energy. Comments on earlier manuscript drafts by Patricia Maurice and James Smith are gratefully acknowledged. We thank Dr. James Dynes for assistance with obtaining reference compounds and Drs. Jian Wang and David Kilcoyne for assistance with operations of STXM5.3.2.

Supporting Information Available

Supplementary methods, Figures S1 and S2, and Table S1. This material is available free of charge via the Internet at http://pubs.acs.org.

Literature Cited

(1) Pace, N. R. A molecular view of microbial diversity and the biosphere. *Science* **1997**, *276*, 734–740.
(2) Raes, J.; Bork, P. Molecular eco-systems biology: Towards an understanding of community function. *Nat. Rev. Microbiol.* **2008**, *6*, 693–699.
(3) Xu, J. Microbial ecology in the age of genomics and metagenomics: Concepts, tools, and recent advances. *Mol. Ecol.* **2006**, *15*, 1713–1731.
(4) Bernier, L.; Warren, L. A. Geochemical diversity in S processes mediated by culture-adapted and environmental-enrichments of *Acidithiobacillus* spp. *Geochim. Cosmochim. Acta* **2007**, *71* (23), 5684–5697.
(5) Warren, L. A.; Norlund, K.; Bernier, L. Microbial thiosulphate reaction arrays: The interactive roles of Fe(III), O_2 and microbial strain on disproportionation and oxidation pathways. *Geobiol.* **2008**, *6*, 461–470.
(6) Orphan, V. J.; House, C. H.; Hinrichs, K. U.; McKeegan, K. D.; DeLong, E. F. Methane-consuming archaea revealed by directly coupled isotopic and phylogenetic analysis. *Science.* **2001**, *293* (5529), 484–487.
(7) Cole, A. C.; Semmens, M. J.; LaPara, T. M. Stratification of activity and bacterial community structure in biofilms grown on membranes transferring oxygen. *Appl. Environ. Microb.* **2004**, *70*, 1982–1989.
(8) Wolin, M. J. *Hydrogen Transfer in Microbial Communities: Microbial Interactions and Communities*; Academic Press: London, 1982.
(9) Nordstrom, D. K.; Southam, G. Geomicrobiology of sulphide mineral oxidation. *Rev. Min.* **1997**, *35*, 361–390.
(10) Bernier, L.; Warren, L. A. Microbially driven acidity generation in a tailings lake. *Geobiol.* **2005**, *3* (2), 115–133.
(11) Li, S.-L.; Calmels, D.; Han, G.; Gaillardet, J.; Liu, C.-Q. Sulfuric acid as an agent of carbonate weathering constrained by $\delta^{13}C_{DIC}$: Examples from southwest China. *Earth Planet. Sci. Letts.* **2008**, *270* (3−4), 189–199.
(12) Lerman, A.; Wu, L.; Mackenzie, F. T. CO_2 and H_2SO_4 consumption in weathering and material transport to the ocean, and their role in the global carbon balance. *Mar. Chem.* **2007**, *106* (1−2), 326–350.
(13) Schippers, A.; Jozsa, P. G.; Sand, W. Sulfur chemistry in bacterial leaching of pyrite. *Appl. Environ. Microbiol.* **1996**, *62* (9), 3424–3431.
(14) Suzuki, I. Oxidation of inorganic sulphur compounds: Chemical and enzymatic reactions. *Can. J. Microbiol.* **1999**, *45* (2), 97–105.
(15) Hitchcock, A. P.; et al. Soft X-ray spectromicroscopy of biological and synthetic polymer systems. *J. Electron Spectrosc. Relat. Phenom.* **2005**, *144−147*, 259–269.
(16) Ade, H.; Hitchcock, A. P. NEXAFS microscopy and resonant scattering: Composition and orientation probed in real and reciprocal space. *Polymer* **2008**, *49* (3), 643–675.
(17) Kilcoyne, A. L. D.; Steele, W. F.; Fakra, S.; Hitchcock, P.; Franck, K.; Anderson, E.; Harteneck, B.; Rightor, E. G.; Mitchell, G. E.; Hitchcock, A. P.; Yang, L.; Warwick, T.; Ade, H. Interferometrically controlled scanning transmission microscopes at the Advanced Light Source. *J. Synchrotron Radiat.* **2003**, *10*, 125–136.
(18) Kaznatcheev, K. V.; Karunakaran, C.; Lanke, U. D.; Urquhart, S. G.; Obst, M.; Hitchcock, A. P. Soft X-ray spectromicroscopy beamline at the CLS: Commissioning results. *Nucl. Inst. Meth. A* **2007**, *582* (1), 96–99.
(19) Warwick, T.; Ade, H.; Kilcoyne, A. L. D.; Kritscher, M.; Tylisczcak, T.; Fakra, S.; Hitchcock, A. P.; Hitchcock, P.; Padmore, H. A. A new bend magnet beam line for scanning transmission X-ray microscopy at the Advanced Light Source. *J. Synchrotron Radiat.* **2002**, *9*, 254–257.
(20) Warwick, T.; Andresen, N.; Comins, J.; Kaznacheyev, K.; Kortright, J. B.; McKean, J. P.; Padmore, H. A.; Shuh, D. K.; Stevens, T.; Tyliszczak, T. New implementation of an SX700 undulator beamline at the Advanced Light Source. *AIP Conference Proceedings* **2004**, *705*, 458–461.
(21) Hay, S. J.; Metson, J. B.; Hyland, M. M. Sulfur speciation in aluminum smelting anodes. *Ind. Eng. Chem. Res.* **2004**, *43* (7), 1690–1700.
(22) Peccia, J.; Marchand, E. A.; Silverstein, J.; Hernandez, M. Development and application of small-subunit rRNA probes for the assessment of selected *Thiobacillus* species and members of the genus *Acidiphilium*. *Appl. Environ. Microb.* **2000**, *66* (7), 3065–3072.
(23) Steudel, R.; Holdt, G.; Gobel, T.; Hazeu, W. Sulphur-compounds. 106. Chromatographic-separation of higher polythionates $S_nO_6^{2-}$ (n = 3−22) and their detection in cultures of *Thiobacillus ferrooxidans*: Molecular composition of bacterial sulphur secretions. *Angew. Chem., Int. Edit.* **1987**, *99* (2), 143–146.
(24) Hazeu, W.; Batenburgvandervegte, W. H.; Bos, P.; Vanderpas, R. K.; Kuenen, J. G. The production and utilization of intermediary elemental sulphur during the oxidation of reduced sulphur-compounds by *Thiobacillus ferrooxidans*. *Arch. Microbiol.* **1988**, *150* (6), 574–579.
(25) Prange, A.; Chauvistre, R.; Modrow, H.; Hormes, J.; Truper, H. G.; Dahl, C. Quantitative speciation of sulphur in bacterial sulphur globules; X-ray absorption spectroscopy reveals at least three different species of sulphur. *Microbiol-SGM.* **2002**, *148*, 267–276.
(26) George, G. N.; Pickering, I. J.; Yu, E. Y.; Prince, R. C. X-ray absorption spectroscopy of bacterial sulphur globules. *Microbiol-SGM.* **2001**, *148*, 2267–2268.
(27) Knickerbocker, C.; Nordstrom, D. K.; Southam, G. The role of "blebbing" in overcoming the hydrophobic barrier during biooxidation of elemental sulphur by *Thiobacillus thiooxidans*. *Chem. Geol.* **2000**, *169* (3−4), 425–433.
(28) Zhang, Y.; Yang, Y.; Liu, J.; Qiu, G. Isolation, characterization, and phylogenetic analysis of a heterotrophic acidophilic bacterium. *Prog. Mod. Biomed.* **2007**, *12*, 1784–1786.
(29) Johnson, D. B. Biodiversity and ecology of acidophilic microorganisms. *FEMS Microbiol. Ecol.* **1998**, *27* (4), 307–317.
(30) Johnson, D. B.; Kelso, W. I. Detection of heterotrophic contaminants in cultures of *Thiobacillus ferrooxidans* and their elimination by subculturing in media containing copper sulfate. *J. Gen. Microbiol.* **1983**, *129*, 2969–2972.
(31) Marchand, E. A.; Silverstein, J. Influence of heterotrophic microbial growth on biological oxidation of pyrite. *Environ. Sci. Technol.* **2002**, *36* (24), 5483–5490.

ES803616K